Eur. Phys. J. C 43, 345–351 (2005)
Digital Object Identifier (DOI) 10.1140/epjc/s2005-02268-y

THE EUROPEAN PHYSICAL JOURNAL C

Stochastic aspects of QCD at high energy

E. Iancu[a]

Service de Physique Théorique, CEA/DSM/SPhT, Unité de recherche associée au CNRS, CE Saclay, 91191 Gif-sur-Yvette, France

Received: 24 March 2005 /
Published online: 3 June 2005 –

Abstract. I present a pedagogical discussion of the influence of particle number fluctuations on the high energy evolution in QCD. I emphasize the event-by-event description and the correspondence with the problem of "fluctuating pulled fronts" in statistical physics. I explain that the correlations generated by fluctuations reduce the phase space for BFKL evolution up to saturation. Because of that, the evolution slows down, and the rate for the energy increase of the saturation momentum is considerably decreased. I discuss the diagrammatic interpretation of the particle number fluctuations in terms of pomeron loops.

PACS. 05.40.+j,11.55.-m,12.38.Cy,13.60.Hb

1 Introduction

Much of the recent progress in our understanding of QCD evolution at high energy has been triggered by the observations that
(i) the gluon number fluctuations play an important role in the evolution towards saturation and the unitarity limit [1,2] and
(ii) the QCD evolution in the presence of fluctuations and saturation is in the same universality class as a series of problems in statistical physics, the prototype of which being the "reaction–diffusion" problem [3,2,4].

These observations have developed into a profound and extremely fruitful correspondence between QCD at high energy and modern problems in statistical physics, which relates topics of current research in both fields, and which has already allowed us to deduce some insightful results in QCD by properly translating the corresponding results from statistical physics.

At the same time, the recognition of the importance of fluctuations has revived the interest in the dilute regime of QCD at high energy, which has been somehow overlooked by the modern theory for gluon saturation, the color glass condensate [5]. A more appropriate formalism in that respect is Mueller's "color dipole" picture [6], which describes the gluon number fluctuations in the limit where the number of "colors" N_c is large. In fact, it was in the context of this formalism that Salam has first noticed, through numerical simulations [7], the dramatic role played by fluctuations in the course of the evolution.

Thus, not surprisingly, the dipole picture occupies a central role in the recent developments aiming at the inclusion of the effects of particle number fluctuations in the non-linear evolution towards saturation [4,8,9]. Furthermore, the dipole picture will play a crucial role in the presentation we shall give here, and which is largely adapted from [1,2,4,9].

2 The Balitsky–Kovchegov equation

The simplest physical context in which one can address the study of gluon saturation is the collision between a small color dipole (a quark–antiquark pair in a colorless state) and a high energy hadron (the "target"). At high energy, the target wavefunction is dominated by gluons, to which couple the quark and the antiquark in the dipole. Thus, by following the evolution of the dipole scattering amplitude towards the unitarity limit, one can obtain information about the evolution of the gluon distribution in the target towards saturation.

Since the projectile has such a simple structure, it is quite easy to deduce the equation describing the evolution of the corresponding S–matrix with increasing energy. We shall denote the elastic scattering amplitude as $\langle T(\boldsymbol{x},\boldsymbol{y})\rangle_\tau$, where $\boldsymbol{x}$ and $\boldsymbol{y}$ are the transverse coordinates of the quark and the antiquark, respectively, and $\tau \sim \ln s$ is the "rapidity" variable, with s the total invariant energy squared. As we shall see, τ plays the role of an "evolution time" for the quantum evolution with increasing energy. Now suppose we increase τ by a small amount $d\tau$. In order to compute the corresponding change in $\langle T\rangle_\tau$, it is more convenient to keep the rapidity of the target fixed and put the small change of rapidity into the elementary dipole. The latter

[a] Membre du Centre National de la Recherche Scientifique (CNRS), France.
[a] e-mail: iancu@spht.saclay.cea.fr

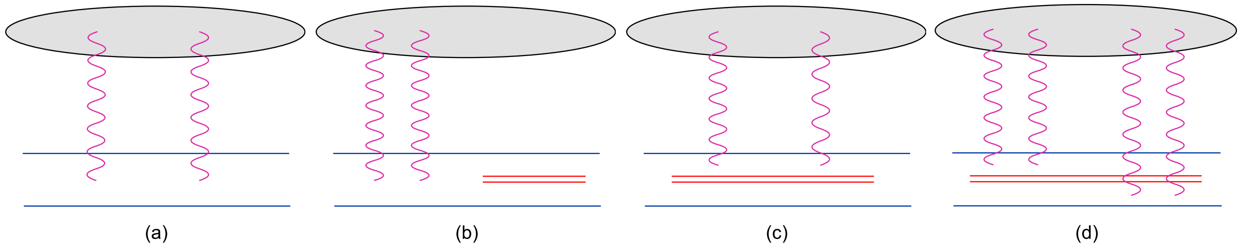

Fig. 1. Diagrams for the evolution of the dipole scattering amplitude, cf. (2): **a** the tree-level contribution; **b** the virtual correction $-\langle T(\boldsymbol{x},\boldsymbol{y})\rangle$; **c** the scattering of one child dipole, $\langle T(\boldsymbol{x},\boldsymbol{z})\rangle$ or $\langle T(\boldsymbol{z},\boldsymbol{y})\rangle$; **d** the simultaneous scattering of both child dipoles, $\langle T^{(2)}(\boldsymbol{x},\boldsymbol{z};\boldsymbol{z},\boldsymbol{y})\rangle$

then "evolves", that is, it has a small probability of emitting a gluon due to this change of rapidity, which can be estimated as

$$\mathrm{d}P = \frac{\alpha_{\mathrm{s}} N_c}{2\pi^2}\,\mathcal{M}(\boldsymbol{x},\boldsymbol{y},\boldsymbol{z})\,\mathrm{d}^2\boldsymbol{z}\,\mathrm{d}\tau\,,$$
$$\mathcal{M}(\boldsymbol{x},\boldsymbol{y},\boldsymbol{z}) \equiv \frac{(\boldsymbol{x}-\boldsymbol{y})^2}{(\boldsymbol{x}-\boldsymbol{z})^2(\boldsymbol{y}-\boldsymbol{z})^2}\,, \tag{1}$$

where N_c is the number of colors and $\boldsymbol{z}$ is the transverse coordinate of the emitted gluon. In the large-N_c limit, to which we shall restrict ourselves in what follows, the gluon can be effectively replaced by a zero-size $q\bar{q}$ pair, and the gluon emission appears as the splitting of the original dipole $(\boldsymbol{x},\boldsymbol{y})$ into two new dipoles $(\boldsymbol{x},\boldsymbol{z})$ and $(\boldsymbol{z},\boldsymbol{y})$.

If the emitted gluon is in the wavefunction of the dipole at the time it scatters on the target, then what scatters is a system of two dipoles. If the gluon is not in the wavefunction at the time of the scattering, it can be viewed as the "virtual" term which decreases the probability that the original quark–antiquark pair remain a simple dipole. The whole process can be summarized into the following evolution equation, which has been originally derived by Balitsky [10]:

$$\frac{\partial}{\partial\tau}\langle T(\boldsymbol{x},\boldsymbol{y})\rangle_\tau = \frac{\bar{\alpha}_{\mathrm{s}}}{2\pi}\int_{\boldsymbol{z}} \mathcal{M}(\boldsymbol{x},\boldsymbol{y},\boldsymbol{z})\,\big\{ -\langle T(\boldsymbol{x},\boldsymbol{y})\rangle_\tau + \langle T(\boldsymbol{x},\boldsymbol{z})\rangle_\tau + \langle T(\boldsymbol{z},\boldsymbol{y})\rangle_\tau - \langle T^{(2)}(\boldsymbol{x},\boldsymbol{z};\boldsymbol{z},\boldsymbol{y})\rangle_\tau \big\}. \tag{2}$$

This equation is illustrated with a few Feynman graphs in Fig. 1. (For simplicity, in this figure we represent the scattering between an elementary dipole and the target in the two-gluon exchange approximation.)

But although formally simple, (2) is not a closed equation – it relates a single-dipole scattering amplitude to a two-dipole one –, and the true difficulty refers to the evaluation of $\langle T^{(2)}\rangle_\tau$. To that aim, we need some information about the target. The simplest approximation is to assume factorization,

$$\langle T^{(2)}(\boldsymbol{x},\boldsymbol{z};\boldsymbol{z},\boldsymbol{y})\rangle_\tau \approx \langle T(\boldsymbol{x},\boldsymbol{z})\rangle_\tau\,\langle T(\boldsymbol{z},\boldsymbol{y})\rangle_\tau\,, \tag{3}$$

which is a mean field approximation (MFA) for the gluon fields in the target. This immediately yields a closed, non-linear, equation for $\langle T\rangle_\tau$:

$$\frac{\partial}{\partial\tau}\langle T(\boldsymbol{x},\boldsymbol{y})\rangle_\tau = \frac{\bar{\alpha}_{\mathrm{s}}}{2\pi}\int_{\boldsymbol{z}} \mathcal{M}(\boldsymbol{x},\boldsymbol{y},\boldsymbol{z})\,\big\{ -\langle T(\boldsymbol{x},\boldsymbol{y})\rangle_\tau + \langle T(\boldsymbol{x},\boldsymbol{z})\rangle_\tau + \langle T(\boldsymbol{z},\boldsymbol{y})\rangle_\tau - \langle T(\boldsymbol{x},\boldsymbol{z})\rangle_\tau\,\langle T(\boldsymbol{z},\boldsymbol{y})\rangle_\tau \big\}. \tag{4}$$

This is the equation originally derived by Kovchegov [11], and is commonly referred as the "Balitsky–Kovchegov (BK) equation". Remarkably, this equation predicts that the scattering amplitude should approach the unitarity bound $T = 1$ in the high energy limit. By contrast, the linearized version of this equation (which is the BFKL equation [12]) predicts an exponential growth of the amplitude with τ, which would eventually violate unitarity. But, of course, the linear approximation breaks down when the average amplitude becomes of order one, since then the non-linear term becomes important and restores unitarity. As manifest on Fig. 1, the non-linear effects reflect multiple scattering.

In what follows we shall be primarily interested in the limitations of (4), coming from the factorization assumption (3). The latter may be a good approximation if the target is a large nucleus and for not very high energies, which is the situation for which Kovchegov has originally derived this equation. More generally, this should work reasonably well when the scattering is sufficiently strong, that is, when $\langle T\rangle_\tau$ is not much smaller than one, because in that case the external dipole scatters off a high-density gluonic system, and the density fluctuations are relatively unimportant. On the other hand, the MFA cannot be right if the scattering is very weak, because then the dipole is sensitive to the dilute part of the target wavefunction, where the fluctuations are, of course, essential. Still, given that our main interest when using (4) is in the strong scattering regime, one may expect the limitations of this equation in the dilute regime to be inessential for the problem at hand. However, this expectation turns out to be incorrect, and this is precisely what we would like to explain in what follows: the particle number fluctuations in the dilute regime have a strong influence, via their subsequent evolution, on the approach towards saturation and the unitarity limit.

3 The fate of the rare fluctuations

Since the fluctuations are a priori important in the weak scattering regime, we shall focus on the scattering of a small dipole, with transverse size $r \equiv |\boldsymbol{x}-\boldsymbol{y}| \ll 1/Q_{\rm s}(\tau)$. We have introduced here the saturation momentum $Q_{\rm s}(\tau)$, which is a characteristic scale of the gluon distribution in the target, and marks the scale at which a dipole scattering off the target makes the transition from weak ($r \ll 1/Q_{\rm s}$) to strong ($r \gg 1/Q_{\rm s}$) interactions. It is in fact common to define $Q_{\rm s}(\tau)$ by the condition

$$\langle T(\boldsymbol{x},\boldsymbol{y})\rangle_\tau = 1/2 \qquad \text{for} \qquad r = 1/Q_{\rm s}(\tau)\,, \tag{5}$$

and to use this condition together with the solution to the BK equation (4) in order to compute the energy dependence of the saturation momentum. We shall discuss more on this in the next section.

Returning to our small external dipole, we would like to relate its scattering amplitude to the average gluon density in the target. This is indeed possible in the dilute regime, since then the dipole scatters only once. In fact, at large N_c we can achieve a more symmetric description by representing also the gluons in the target as color dipoles, with a dipole number density $n(\boldsymbol{u},\boldsymbol{v})$ (for dipoles with a quark at $\boldsymbol{u}$ and an antiquark at $\boldsymbol{v}$). The external dipole $(\boldsymbol{x},\boldsymbol{y})$ can scatter off any of the internal dipoles $(\boldsymbol{u},\boldsymbol{v})$ by exchanging two gluons. This gives

$$\langle T(\boldsymbol{x},\boldsymbol{y})\rangle_\tau = \alpha_{\rm s}^2 \int {\rm d}^2\boldsymbol{u}\,{\rm d}^2\boldsymbol{v}\,\mathcal{A}_0(\boldsymbol{x},\boldsymbol{y}|\boldsymbol{u},\boldsymbol{v})\ \langle n(\boldsymbol{u},\boldsymbol{v})\rangle_\tau\,, \tag{6}$$

where $\alpha_{\rm s}^2\mathcal{A}_0(\boldsymbol{x},\boldsymbol{y}|\boldsymbol{u},\boldsymbol{v})$ is the scattering amplitude for two elementary dipoles. Here, we shall not need its exact expression, but only the fact that it is quasi-local both with respect to the dipole sizes and with respect to their impact parameters. (The impact parameter of a dipole $(\boldsymbol{x},\boldsymbol{y})$ is its center-of-mass coordinate $\boldsymbol{b}=(\boldsymbol{x}+\boldsymbol{y})/2$.) This allows us to simplify (6) as

$$\langle T(r,b)\rangle_\tau \simeq \alpha_{\rm s}^2\,\langle f(r,b)\rangle_\tau\,, \tag{7}$$

where the dimensionless quantity

$$f(r,b) \simeq r^2 \int_\Sigma {\rm d}^2\boldsymbol{b}'\, n(\boldsymbol{r},\boldsymbol{b}') \tag{8}$$

is the dipole occupation number in the target, that is, the number of dipoles with size r (per unit of $\ln r^2$) within an area $\Sigma \sim r^2$ centered at b. Equation (7) shows that a small dipole projectile is a very precise analyzer of the dipole distribution in the target: the external dipoles count the numbers of internal dipoles having the same transverse size and impact parameter as itself.

Equation (7) applies so long as $\langle T\rangle_\tau \ll 1$, but by extrapolation it shows that unitarity corrections in the dipole–target scattering become important when the dipole occupation factor in the target becomes of order $1/\alpha_{\rm s}^2$. This is precisely the critical density at which saturation effects – i.e., non-linear effects in the target wavefunction leading to the saturation of the gluon distribution – are expected to occur [6]. This argument confirms that, by studying dipole scattering in the vicinity of the unitarity limit, one has access to the physics of gluon saturation.

Let us assume an initial condition like (7) at the initial rapidity τ_0 and follow the evolution of the scattering amplitude with increasing τ. At the beginning, the amplitude will rise very fast, according to the BFKL equation, but this rise will be eventually stopped by the non-linear term $\langle T^{(2)}\rangle_\tau \equiv \langle T^{(2)}(\boldsymbol{x},\boldsymbol{z};\boldsymbol{z},\boldsymbol{y})\rangle_\tau$ in (2), which in the linear regime rises even faster. We have, schematically,

$$\langle T\rangle_\tau \simeq T_0\,{\rm e}^{\omega_{\mathbb{P}}(\tau-\tau_0)}\,, \qquad \langle T^{(2)}\rangle_\tau \simeq T_0^{(2)}\,{\rm e}^{2\omega_{\mathbb{P}}(\tau-\tau_0)}\,, \tag{9}$$

where $\omega_{\mathbb{P}} = \text{const.}\times\bar\alpha_{\rm s}$, $T_0 \equiv \langle T\rangle_{\tau_0} \simeq \alpha_{\rm s}^2 f_0$ and $T_0^{(2)} \equiv \langle T^{(2)}\rangle_{\tau_0}$. ($f_0$ denotes the average occupation factor at $\tau=\tau_0$.) The unitarity limit is approached when $\langle T^{(2)}\rangle_\tau \sim \langle T\rangle_\tau$, which in turn implies $\tau\sim\tau_{\rm c}$ with

$${\rm e}^{\omega_{\mathbb{P}}(\tau_{\rm c}-\tau_0)} \sim T_0/T_0^{(2)}\,. \tag{10}$$

So, what is the ratio $T_0^{(2)}/T_0$? If one assumes the factorization property (3), then $T_0^{(2)} \approx (T_0)^2$, and therefore $T_0^{(2)}/T_0 \approx T_0 \simeq \alpha_{\rm s}^2 f_0$. Then (10) implies

$$\tau_{\rm c}-\tau_0 \simeq \frac{1}{\omega_{\mathbb{P}}}\ln\frac{1}{\alpha_{\rm s}^2 f_0} = \frac{1}{\omega_{\mathbb{P}}}\left(\ln\frac{1}{\alpha_{\rm s}^2}+\ln\frac{1}{f_0}\right). \tag{11}$$

But is the MFA (3) a reasonable approximation for a dilute initial condition? To answer this question, let us consider two physical situations:
(i) $f_0 \gg 1$ (with $f_0 \ll 1/\alpha_{\rm s}^2$ though) and
(ii) $f_0 \ll 1$. Also, remember that $\langle T^{(2)}(\boldsymbol{x},\boldsymbol{z};\boldsymbol{z},\boldsymbol{y})\rangle_\tau$ is the scattering amplitude for two incoming dipoles $(\boldsymbol{x},\boldsymbol{z})$ and $(\boldsymbol{z},\boldsymbol{y})$ which have similar impact factors (since they have a common leg at $\boldsymbol{z}$) and also similar sizes (since the QCD evolution, (2), favors the splitting into dipoles with similar sizes).
(i) In the first case, the disk $\Sigma\sim r^2$ at b has a high occupancy, so the two external dipoles will predominantly scatter off different dipoles in that disk. Then, their scatterings are largely independent, and the MFA is reasonable. The result (11) can thus be trusted in this case.
(ii) The statement that the average occupation factor f_0 is much smaller than one requires an explanation. Clearly, in a given configuration of the target, the occupation number (8) is discrete: $f=0,1,2,\ldots$; so, for its average value to be smaller than one, one needs to look at rare configurations. That is, if one considers the statistical ensemble of dipole configurations generated by the evolution up to rapidity τ_0, then for most of these configurations $f(r,b)=0$, but for a small fraction among them, of order f_0, f is non-zero and of order one. Thus, f_0 is essentially the probability to find a dipole with the required characteristics (r,b) in the ensemble.

Consider now the scattering problem in such a very dilute regime: the fact that $T_0 \sim \alpha_{\rm s}^2 f_0 \ll \alpha_{\rm s}^2$ means that the incoming dipole (r,b) has a small probability $f_0(r,b)$ to find a dipole with similar characteristics in the target, with which it then interacts with a strength $\alpha_{\rm s}^2$. Consider now two incoming dipoles, with similar sizes and impact parameters: there is a small probability $f_0(r, b)$ to find a corresponding dipole in the target, but whenever this happens, both external dipoles can scatter off it, with an overall strength α_s^4. This gives $T_0^{(2)} \sim \alpha_s^4 f_0 \sim \alpha_s^2 T_0$, which is much larger than the MFA prediction $T_0^{(2)} \sim (T_0)^2$. The scattering of the external dipoles is now strongly correlated. With this estimate for $T_0^{(2)}$, (10) implies

$$\tau_c - \tau_0 \simeq \frac{1}{\omega_{\mathbb{P}}} \ln \frac{1}{\alpha_s^2} \,. \qquad (12)$$

For $f_0 \ll 1$, this is considerably smaller than the naive estimate (11) based on the MFA. Thus, by enhancing the correlations in the dilute regime, the fluctuations in the particle number significantly reduce the rapidity window for BFKL evolution.

Moreover, at the rapidity τ_c at which the unitarity corrections cut off the BFKL growth, (9) and (12) imply $\langle T\rangle_{\tau_c} \sim \langle T^{(2)}\rangle_{\tau_c} \sim f_0 \ll 1$, in sharp contrast with the prediction of the MFA! That is, the contribution that a rare fluctuation (r, b) at $\tau = \tau_0$ can give, through its subsequent evolution, to the average amplitude $\langle T(r, b)\rangle_\tau$ at $\tau > \tau_0$, saturates at a value smaller than one (of the order of the probability $f_0(r, b) \ll 1$ of the original fluctuation) [1]. Besides, this contribution violates the factorization assumption implicit in the BK equation [4].

We conclude that the correlations in the dilute regime significantly reduce the phase space available for the BFKL evolution of the average amplitude towards saturation, by eliminating the rare fluctuations (r, b) for which $\langle f(r, b)\rangle_\tau < 1$, or, equivalently, for which $\langle T(r, b)\rangle_\tau < \alpha_s^2$ [1]. The limiting value α_s^2 is the elementary "quantum" for the strength of T in the event-by-event description, that is, the minimal non-trivial value that a physical scattering amplitude can take in a particular event, where the dipole number is discrete [2].

In view of this, one expects the evolution to "slow down" as compared to the MFA. This is confirmed by an original calculation by Mueller and Shoshi [1], which shows that the rate for the growth of saturation momentum with the energy is considerably reduced as compared to the MFA. In the next section, we shall recover the result of [1] from a broader perspective, which establishes a remarkable correspondence with modern results in statistical physics [2].

4 Fluctuating pulled fronts

To perform a detailed study of the influence of fluctuations on the evolution towards high density, one needs a theory for correlations like $\langle T^{(2)}\rangle_\tau$ in the presence of fluctuations. Such a theory has been recently given (within the large-N_c approximation) [4,9,8], and we shall briefly comment on it in the last section. But before doing that, we would like to show that some very general results concerning the effects of fluctuations can be deduced without a detailed knowledge of the microscopic dynamics, by relying on universal results from statistical physics [2].

Specifically, the only assumptions that we shall need in order to derive these results are the following:
(i) the mean field description of the dynamics of $\langle T\rangle_\tau$ is provided by the BK equation (4), and
(ii) in the event-by-event description, the amplitude T is a discrete quantity, with step $\Delta T \sim \alpha_s^2$.

We start by summarizing those results about the BK equation that are needed for the present purposes. We shall neglect the impact parameter dependence of the amplitude, and write the corresponding solution as $\langle T(r)\rangle_\tau \equiv \overline{T}_\tau(\rho)$, where $\rho \equiv \ln(r_0^2/r^2)$ and r_0 is a scale introduced by the initial conditions at low energy. Note that small dipole sizes correspond to large values of ρ. Thus, the amplitude is small, $\overline{T}_\tau(\rho) \ll 1$, when ρ is sufficiently large: $\rho \gg \bar{\rho}_s(\tau)$, where $\bar{\rho}_s(\tau) \equiv \ln(r_0^2 \bar{Q}_s^2(\tau))$ and $\bar{Q}_s^2(\tau)$ denotes the saturation momentum extracted from the BK equation.

The solution $\overline{T}_\tau(\rho)$ can be visualized as a front which interpolates between $T = 1$ (the unitarity limit) at $\rho \to -\infty$ and $T = 0$ at $\rho \to \infty$ [3]. Note that $T = 1$ and $T = 0$ are stable and, respectively, unstable fixed points of the BK equation. The transition between the two regimes occurs at $\rho \sim \bar{\rho}_s(\tau)$; thus, the (logarithm of the) saturation momentum plays the role of the position of the front. With increasing τ, the saturation momentum rises very fast (exponentially in τ), so the front moves towards larger values of ρ. One finds [13–15,3]

$$Q_s^2(\tau) \simeq Q_0^2 \, \frac{e^{c\bar{\alpha}_s \tau}}{(\bar{\alpha}_s \tau)^{3/2\gamma_s}} \,, \qquad (13)$$

where $Q_0^2 \propto 1/r_0^2$, and c and γ_s are numbers fixed by the BFKL dynamics: $c = 4.88...$ and $\gamma_s = 0.63...$ Equation (13) implies the following expression for the front velocity:

$$\bar{\lambda}(\tau) \equiv \frac{d\bar{\rho}_s(\tau)}{d\tau} \simeq c\bar{\alpha}_s - \frac{3}{2\gamma_s} \frac{1}{\tau} \,. \qquad (14)$$

Its asymptotic value at large τ represents the saturation exponent (the rate for the exponential growth of $Q_s^2(\tau)$), here estimated in the MFA: $\bar{\lambda}_{as} = c\bar{\alpha}_s$.

In the weak scattering (dilute) regime at $\rho \gg \bar{\rho}_s(\tau)$, the form of the amplitude can be obtained by solving the linearized version of (4), that is, the BFKL equation. One thus finds [14,15,3]:

$$\overline{T}_\tau(\rho) \simeq (\rho - \bar{\rho}_s) \, e^{-\gamma_s(\rho - \bar{\rho}_s)} \, \exp\left\{ -\frac{(\rho - \bar{\rho}_s)^2}{2\beta\bar{\alpha}_s\tau} \right\} \qquad (15)$$

(with $\beta \simeq 48.2$). In particular, so long as the difference $\rho - \bar{\rho}_s$ remains much smaller than the diffusion radius $\sim \sqrt{2\beta\bar{\alpha}_s\tau}$, the Gaussian in (15) can be ignored, and the amplitude becomes purely a function of $\rho - \bar{\rho}_s(\tau)$:

$$\overline{T}_\tau(\rho) \simeq (\rho - \bar{\rho}_s(\tau)) \, e^{-\gamma_s(\rho - \bar{\rho}_s(\tau))} \,, \qquad (16)$$

valid for $\rho - \bar{\rho}_s \ll \sqrt{2\beta\bar{\alpha}_s\tau}$. This is the property referred to as "geometric scaling" [16,14]. It means that the front propagates without distortion, as a traveling wave [3].

Notice the mechanism leading to the front propagation: For a fixed $\rho \gg \bar{\rho}_s(\tau)$, the amplitude (15) rises

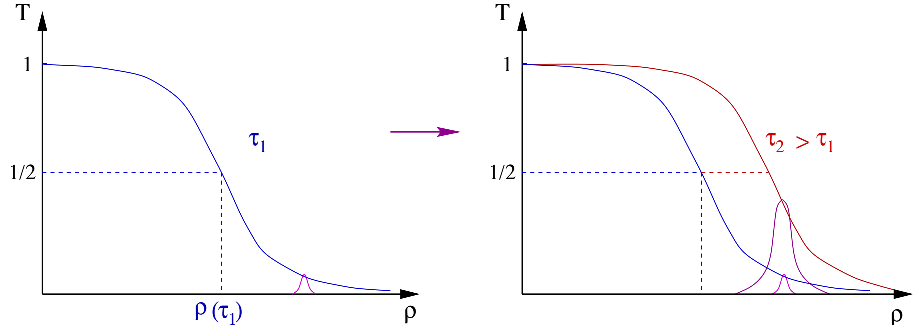

Fig. 2. Evolution of the continuum front of the BK equation with increasing rapidity τ

rapidly with τ, due to the exponential factor $\exp(\gamma_s \bar{\rho}_s) \simeq e^{\omega_{\mathbb{P}}\tau}$ with $\omega_{\mathbb{P}} = \gamma_s \bar{\lambda}_{as}$; this is the BFKL instability (see Fig. 2). Thus the front is pulled by the unstable (BFKL) growth of its tail at large ρ. Besides, for a given (large) distance $\rho - \bar{\rho}_s$ ahead of the front, the amplitude increases through diffusion from smaller values of ρ, until it reaches the profile (16) of the traveling wave.

The fact that the front corresponding to the BK equation is a pulled front – it propagates via the growth and spreading of small perturbations around the unstable state $T = 0$ – is crucial for the problem at hand, as it shows that the front dynamics is driven by its leading edge (the front region where $T \ll 1$), and therefore it might be very sensitive to fluctuations. Although this property has been discussed here on the basis of the linear, BFKL, equation, it turns out that this is an exact property of the non-linear BK equation [3]. Indeed, as shown by Munier and Peschanski, the BK equation is in the same universality class as the Fisher–Kolmogorov–Petrovsky–Piscounov (FKPP) equation [17], which appears as a mean field approximation to a variety of stochastic problems in chemistry, physics, and biology, and for which the pulled front property has been rigorously demonstrated (see [18,19] for recent reviews and more references).

Let us now return to the actual microscopic dynamics, which is stochastic (it includes fluctuations in the number of dipoles in the target), and where the scattering amplitude (in a given event) is discrete. Then, as discussed in the previous section, one needs to consider a statistical ensemble of configurations which correspond to different realizations of the same evolution. To any of these configurations one can associate a front $T_\tau(\rho)$, which characterizes the scattering between that particular configuration and external dipoles of arbitrary size ρ.

As in the mean field case, the evolution of a configuration is described as the propagation of the associated front towards larger values of ρ. What is however new is that, because of discreteness, a microscopic front looks like a histogram: T_τ and ρ are now discrete quantities, with steps $\Delta T = \alpha_s^2$ and $\Delta \rho = 1$, respectively. Because of that, the front is necessarily compact – for any τ, there is only a finite number of bins in ρ ahead of ρ_s where T_τ is non-zero (see Fig. 3) –, and this property turns out to have dramatic consequences for the propagation of the front:

In the empty bins on the right of the front tip, the local, BFKL, growth is not possible anymore (this would require a seed!). Thus, the only way for the front to progress there is via diffusion, i.e., via radiation from the occupied bins at $\rho < \rho_{tip}$ (see Fig. 3). But since diffusion is less effective than the local growth, we expect the velocity of the front – which is also the saturation exponent – to be reduced for the microscopic front as compared to the front of the MFA. The difference between the mechanisms for front propagation in the MFA and in a microscopic event can be also appreciated by comparing Figs. 2 and 3.

The extreme sensitivity of the pulled fronts to small fluctuations has been recognized in the context of statistical physics only in the recent years [20,19]. The discrete particle version of a pulled front is generally referred to as a "fluctuating pulled front" [18,19]. The most striking feature of such a system is that the convergence towards the mean field limit is extremely slow, logarithmic in the maximal occupation number N. (For QCD, $N \sim 1/\alpha_s^2$, as explained after (8).) Specifically, if λ_N denotes the velocity of the microscopic front for a finite value of N, and λ_∞ is the respective velocity in the MFA (which corresponds to the limit $N \to \infty$), then for $N \gg 1$ one finds $v_N \simeq v_0 - \mathcal{C}/\ln^2 N$, where $\mathcal{C}$ is a constant.

An analytic argument which explains this slow convergence and allows one to compute $\mathcal{C}$ has been given by Brunet and Derrida [20]. Rather than reproducing the original derivation from [20], we prefer to present (directly for the case of QCD) a qualitative argument which explains the most salient feature of their result, namely its slow convergence to the mean field limit as $N \to \infty$.

This is related to the fact that, as mentioned before, the microscopic front has a compact width, and therefore its evolution is frozen in a state of "pre-asymptotic velocity" [2]. The width of the front is the distance $\Delta\rho_f = \rho - \rho_s$ over which the amplitude $T_\tau(\rho)$ decreases from $T_\tau(\rho_s) \sim 1$ down the minimal allowed value $T \sim \alpha_s^2$. This can be estimated from (16) as $\Delta\rho_f \sim (1/\gamma_s) \ln(1/\alpha_s^2)$.

Now, from the discussion after (16) we know that the front sets in diffusively and thus requires a formation "time": (15) shows that, for the front to spread over a given distance $\rho - \rho_s$, it takes a rapidity evolution

$$\bar{\alpha}_s \, \tau \sim \frac{(\rho - \rho_s)^2}{2\beta} \,. \qquad (17)$$

Through this evolution, the velocity of the front increases towards its asymptotic value according to (14). If the front is allowed to extend arbitrarily far away, as it was the case for the MFA, then the velocity will asymptotically

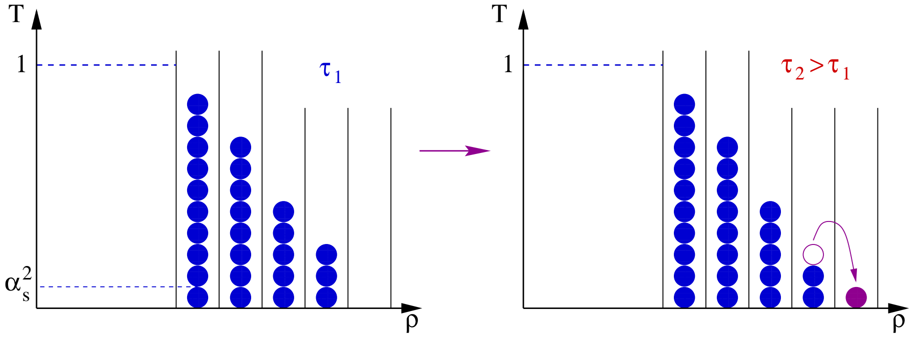

Fig. 3. Evolution of the discrete front of a microscopic event with increasing rapidity τ. The small blobs are meant to represent the elementary quanta α_s^2 of T in a microscopic event

approach the value $\bar{\lambda}$. However, when the front is compact, as for the discrete system, the formation time is finite as well, namely of the order

$$\bar{\alpha}_s \Delta\tau \sim \frac{(\Delta\rho_f)^2}{2\beta} \sim \frac{\ln^2(1/\alpha_s^2)}{2\beta\,\gamma_s^2}\,, \tag{18}$$

which implies that the front velocity cannot increase beyond a value

$$\lambda_{as} \simeq \bar{\lambda}_{as} - \kappa\,\bar{\alpha}_s\,\frac{\gamma_s\beta}{\ln^2(1/\alpha_s^2)}\,. \tag{19}$$

This estimate is valid when $\alpha_s^2 \ll 1$. The fudge factor κ cannot be determined by this qualitative argument, but this is computed in [20] as $\kappa = \pi^2/2$.

The first term in (19) is the mean field estimate $\bar{\lambda}_{as} \simeq 4.88\bar{\alpha}_s$. But the second, corrective, term is particularly large, not only because it decreases very slowly with α_s^2, but also because its coefficient is numerically large: $\pi^2\gamma_s\beta/2 \approx 150$. Thus, although (19) becomes an exact result when α_s^2 is arbitrarily small, this result remains useless for practical applications.

5 Pomeron loops

So far, our discussion has been mostly qualitative, and the language used was essentially that of statistical physics. But it is also interesting to understand these results within the more traditional language of perturbative QCD, that is, in terms of Feynman graphs and evolution equations. This is especially important in view of the limitations of the correspondence with the statistical physics, which so far has only allowed us to obtain asymptotic results (valid when $\bar{\alpha}_s\tau \to \infty$ and $\alpha_s^2 \to 0$) like (19). To go beyond these results, we need the actual evolution equations in QCD in the presence of both fluctuations and saturation. These equations have been constructed in the large-N_c limit [4,8,9], by combining the Balitsky equations (or the CGC formalism) in the high density regime with the dipole picture in the dilute regime. To motivate the structure of these equations, we shall first discuss the diagrammatic interpretation of the particle number fluctuations.

We shall use, as before, the dipole picture for the target wavefunction in the dilute regime. Then, fluctuations in the dipole number appear because of the possibility that one dipole internal to the target splits into two dipoles in one step of the evolution. In the discussion of (2) we have already shown, in Fig. 1, the basic diagram for dipole splitting. In that discussion, the dipole appeared as the projectile, and the evolution was viewed as projectile evolution (that is, the small rapidity increment $\mathrm{d}\tau$ was given to the projectile). Here, we would like to visualize the relevant fluctuations as splittings of the elementary dipoles inside the target, and to that aim we need to perform target evolution.

In Fig. 4 we show one step in the evolution of the target, in which one of the dipoles there – the one with legs at $\boldsymbol{u}$ and $\boldsymbol{v}$ – has split into two new dipoles (with coordinates $(\boldsymbol{u},\boldsymbol{z})$ and $(\boldsymbol{z},\boldsymbol{v})$, respectively). As further illustrated there, the original dipole can be probed via scattering with one external dipole $(\boldsymbol{x},\boldsymbol{y})$, in which case it provides a contribution to the scattering amplitude $\langle T(\boldsymbol{x},\boldsymbol{y})\rangle_\tau$ at the original rapidity τ. After evolution, the two child dipoles can be measured via the scattering with two external dipoles, thus giving a contribution to the respective amplitude $\langle T^{(2)}(\boldsymbol{x}_1,\boldsymbol{y}_1;\boldsymbol{x}_2,\boldsymbol{y}_2)\rangle_{\tau+\mathrm{d}\tau}$ at rapidity $\tau+\mathrm{d}\tau$. This is in agreement with the discussion in Sect. 3

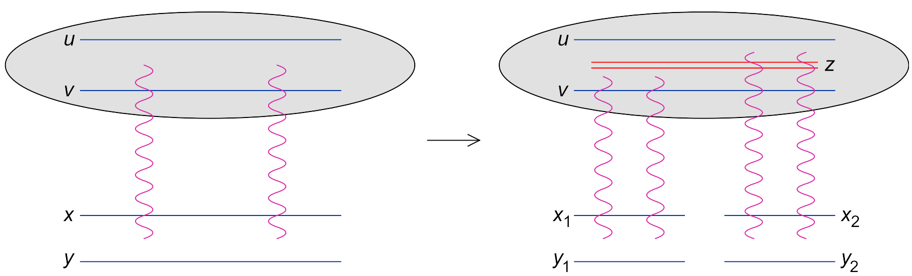

Fig. 4. Target evolution in one step: the original dipole $(\boldsymbol{u},\boldsymbol{v})$ splits into two new dipoles $(\boldsymbol{u},\boldsymbol{z})$ and $(\boldsymbol{z},\boldsymbol{v})$, which then scatter off two external dipoles

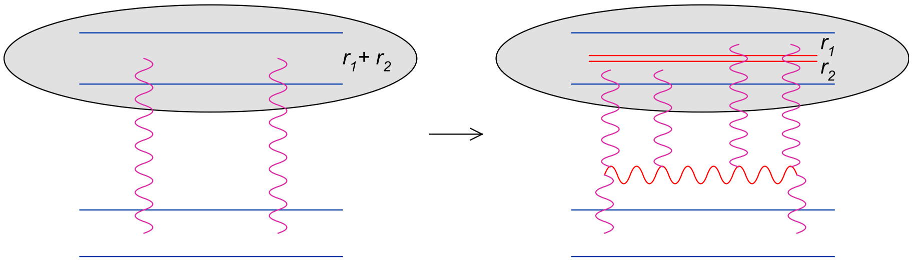

Fig. 5. Two steps in the evolution of the average scattering amplitude of a single dipole: the original amplitude (left) and the pomeron loop generated after two steps (right)

where we have seen that one needs to scatter two external dipoles in order to be sensitive to fluctuations.

From the previous discussion, one can also understand what should be the role of the process in Fig. 4 in the evolution of the scattering amplitudes for external dipoles: this process generates a change in the two-dipole scattering amplitude $\langle T^{(2)} \rangle_\tau$ which is proportional to single-dipole amplitude $\langle T \rangle_\tau$.

Let us finally consider the evolution of the dipole scattering amplitude $\langle T \rangle$ after two steps. This involves several processes, but the most interesting among them is the one displayed in Fig. 5, which is sensitive to both fluctuations and saturation. Specifically, the first step of the evolution is the same as in Fig. 4: one dipole in the target wavefunction splits into two, which implies that $\langle T \rangle$ evolves into a $\langle T^{(2)} \rangle$. In the second step, the $\langle T^{(2)} \rangle$ evolves back into a $\langle T \rangle$, according to the non-linear term in (2). The latter process has been already represented from the perspective of projectile evolution in Fig. 1d. In the lower half part of Fig. 5, this process is now represented as target evolution: From this perspective, it describes the merging of four gluons into two. Altogether, the two-step evolution depicted in Fig. 5 generates a pomeron loop: This involves two "vertices" – one for dipole splitting, the other one for gluon merging – and two "propagators" – one for each dipole–dipole scattering amplitude $\alpha_s^2 \mathcal{A}_0$. An explicit expression for this loop can be found in [21].

References

1. A.H. Mueller, A.I. Shoshi, Nucl. Phys. B **692**, 175 (2004)
2. E. Iancu, A.H. Mueller, S. Munier, Phys. Lett. B **606**, 342 (2005)
3. S. Munier, R. Peschanski, Phys. Rev. Lett. **91**, 232001 (2003)
4. E. Iancu, D.N. Triantafyllopoulos, hep-ph/0411405
5. E. Iancu, R. Venugopalan, in Quark-Gluon Plasma 3, edited by R.C. Hwa, X.-N. Wang (World Scientific, 2003) [hep-ph/0303204]
6. A.H. Mueller, Nucl. Phys. B **415**, 373 (1994); A.H. Mueller, B. Patel, Nucl. Phys. B **425**, 471 (1994); A.H. Mueller, Nucl. Phys. B **437**, 107 (1995)
7. G.P. Salam, Nucl. Phys. B **449**, 589 (1995); **461**, 512 (1996)
8. A.H. Mueller, A.I. Shoshi, S.M.H. Wong, hep-ph/0501088
9. E. Iancu, D.N. Triantafyllopoulos, hep-ph/0501193 (to appear in Phys. Lett. B)
10. I. Balitsky, Nucl. Phys. B **463**, 99 (1996)
11. Yu.V. Kovchegov, Phys. Rev. D **60**, 034008 (1999); D **61**, 074018 (2000)
12. L.N. Lipatov, Sov. J. Nucl. Phys. **23**, 338 (1976); E.A. Kuraev, L.N. Lipatov, V.S. Fadin, Zh. Eksp. Teor. Fiz **72**, 3 (1977) (Sov. Phys. JETP **45**, 199 (1977)); Ya.Ya. Balitsky, L.N. Lipatov, Sov. J. Nucl. Phys. **28**, 822 (1978)
13. L.V. Gribov, E.M. Levin, M.G. Ryskin, Phys. Rept. **100**, 1 (1983)
14. E. Iancu, K. Itakura, L. McLerran, Nucl. Phys. A **708**, 327 (2002)
15. A.H. Mueller, D.N. Triantafyllopoulos, Nucl. Phys. B **640**, 331 (2002)
16. A.M. Stasto, K. Golec-Biernat, J. Kwiecinski, Phys. Rev. Lett. **86**, 596 (2001)
17. R.A. Fisher, Ann. Eugenics **7**, 355 (1937); A. Kolmogorov, I. Petrovsky, N. Piscounov, Moscou Univ. Bull. Math. A **1**, 1 (1937)
18. W. Van Saarloos, Phys. Rep. **386**, 29 (2003)
19. D. Panja, Phys. Rep. **393**, 87 (2004)
20. E. Brunet, B. Derrida, Phys. Rev. E **56**, 2597 (1997); Comp. Phys. Comm. **121–122**, 376 (1999); J. Stat. Phys. **103**, 269 (2001)
21. J.-P. Blaizot, E. Iancu, K. Itakura, D.N. Triantafyllopoulos, hep-ph/0502221